

# Profiles of the Resonance Doublets Formed in Bipolar Winds in Symbiotic Stars

Jerry Jaiyul Yoo<sup>1\*</sup>, Hee-Won Lee<sup>2</sup> and Sang-Hyeon Ahn<sup>3</sup>

<sup>1</sup>*Department of Astronomy, Seoul National University, Shillim-Dong, Kwanak-Gu, Seoul, Korea*

<sup>2</sup>*Department of Geoinformation Science, Sejong University, Gunja-Dong, Gwangjin-Gu, Seoul, Korea*

<sup>3</sup>*Korea Institute for Advanced Study, Cheongyangri-Dong, Dongdaemun-Gu, Seoul, Korea*

Accepted 2002 April 17. Received 2002 March 20; in original form 2002 January 5

## ABSTRACT

We compute the profiles of resonance doublet lines ( $S_{1/2} - P_{1/2,3/2}$ ) formed in bipolar winds with velocity greater than the doublet separation in symbiotic stars. Particular attention has been paid on the doublet line ratio, where an essential role is played by the conversion of the short wavelength component arising from the  $S_{1/2} - P_{3/2}$  transition into the long wavelength component for the transition  $S_{1/2} - P_{1/2}$ . We adopted a Monte Carlo technique and the Sobolev approximation. Our bipolar winds take the form of a cone and are characterized by the terminal wind velocity, the mass loss rate and the opening angle of the cone. When an observer is in the polar direction and the Sobolev optical depth  $\tau_{Sob} \simeq 1$ , we mainly obtain profiles with inverted flux line ratios, where the short wavelength component is weaker than the long wavelength component. When an observer is in the equatorial direction, we find that the profiles are characterized by two broad components, where the long wavelength component is the broader and stronger of the two. We conclude that the profiles obtained in our model provide a qualitative understanding of broad profiles and inverted intensity ratios of the doublets in symbiotic stars.

**Key words:** line: formation — line: profiles — radiative transfer — scattering — binaries: symbiotic — stars: winds, outflows

## 1 INTRODUCTION

Symbiotic stars are generally known to be interacting binaries consisting of a red giant (or a Mira-type variable) and a hot companion that is usually a white dwarf (e.g. Kenyon 1986). Most red giant components suffer a heavy mass loss in the form of a slow stellar wind with a typical terminal speed  $10 \sim 20 \text{ km s}^{-1}$  that is comparable to the escape velocity of a giant (e.g. Schmid 1996). In contrast, many white dwarf systems including planetary nebulae are known to possess fast outflows with terminal speed  $\geq 1000 \text{ km s}^{-1}$ . Similar fast winds are also known in some symbiotic stars including AG Peg (Vogel & Nussbaumer 1994).

The orbital elements of symbiotic stars are not well-constrained, but light curves often show that they possess a long period of several hundred days (e.g. Iben & Tutukov 1996). Mürset & Schmid (1999) presented the relation between the spectral types of the cool giants and the orbital periods to reveal that almost all symbiotic stars are well-detached binary systems. Therefore the most important binary activity may be found from the interaction between

the two different kind of winds. These two winds may collide forming a shocked region, which can be identified with X-ray observations and is consistent with the fact that several symbiotic stars are known to be X-ray sources (Girard & Wilson 1987, Mürset, Wolff & Jordan 1997, Ezuka, Ishida & Makino 1998)

In many symbiotic stars the Raman-scattered O  $\nu_1$   $\lambda\lambda 6827, 7088$  features exhibit multiple peak profiles and strong polarization accompanied by the polarization flip (Schmid 1989, Schmid & Schild 1994, Harries & Howarth 1996). Lee & Park (1999) proposed that these features can be explained by assuming that there is an accretion disk around the white dwarf formed through capture of the slow wind from the giant (e.g. Mastrodemos & Morris 1998). According to the theoretical modelling by Paczynski & Zytkov (1978), periodic hydrogen shell flashes may occur in a white dwarf with the accretion rate  $10^{-11} - 10^{-7} M_{\odot} \text{ yr}^{-1}$ , where each outburst may last for decades. With this eruption the radiative pressure will drive a stellar wind around a white dwarf, which may take a bipolar form subject to the circumstellar matter distribution (Soker & Rappaport 2000). This interpretation is interesting because most symbiotic stars with known nebular morphologies are bipolar (Cor-

\* E-mail: jyyu@astro.snu.ac.kr

radi 1995). Currently it is very controversial whether bipolar planetary nebulae possess central binary systems (e.g. Soker 1998).

It is, therefore, very interesting and important to investigate the line profiles that indicate the fast outflowing motion, from which we may find the physical properties associated with the bipolarity of the wind. Since the resonance doublets arise from the common electronic transitions  $S_{1/2} - P_{1/2,3/2}$  and have the separation ranging from  $500 \text{ km s}^{-1}$  (for C IV) to  $1,650 \text{ km s}^{-1}$  (for O VI), these lines can be an excellent tool to investigate the outflowing hot wind around the white dwarf component.

When the bulk velocity changes significantly in a region that is much smaller than the scale height of the physical quantities such as density, the radiative transfer can be described by the Sobolev approximation. In this case, the optical depth for a line photon is inversely proportional to the velocity gradient in the direction of the photon propagation (e.g. Sobolev 1947; Rybicki & Hummer 1978). In the case of resonance doublet lines, line photons arising from the  $S_{1/2} - P_{3/2}$  transition will be resonantly scattered with  $S_{1/2} - P_{1/2}$  transition by receding ions with the speed of the doublet separation, if the outflow is an accelerating wind with a speed larger than the doublet separation. We denote this type of scattering by ‘double scattering.’ This double scattering converts line photons associated with the  $S_{1/2} - P_{3/2}$  transition into line photons associated with the  $S_{1/2} - P_{1/2}$  transition. This will change the intrinsic doublet line ratio, which is 2 : 1 in the optically thin limit and 1 : 1 in the optically thick limit. Olson (1982) investigated this problem and applied to stellar winds around O and B stars. His main concern was limited to the investigations of various P Cygni profiles in spherical winds.

*IUE* observations indicate that many objects including symbiotic stars and planetary nebulae show various doublet line ratios between 2 : 1 and 1 : 1 (Feibelman 1983, Schmid et al. 1999). The microphysical processes that lead to these various line ratios may be associated with the existence of dust and/or collisional de-excitation (Ahn & Lee 2002, in preparation).

Michalitsianos et al. (1988) showed that some symbiotic stars including RX Pup and R Aqr show anomalous line ratios, in which the short wavelength component of the C IV doublet was observed to be weaker than the long wavelength component. Vogel & Nussbaumer (1994) showed that the symbiotic nova AG Peg exhibits broad He II emission lines that are formed in a fast wind. In this system, the resonance doublets N V and C IV exhibit inverted line ratios where the short wavelength component is weaker. The authors proposed that the line formation is strongly affected by the double scatterings, whereby significant fraction of photons are converted. Furthermore, the doublets did not display P Cygni profiles. These facts imply that the outflowing motion is confined to specific directions (plausibly in the polar directions), which exclude the observer’s line of sight.

There have been many theoretical investigations on the P Cygni profiles shown in the resonance lines of metal elements by adopting the Sobolev approximation. However, relatively little attention has been paid on the profiles observed outside the wind flowing direction. In this paper, we perform Sobolev Monte Carlo computations to obtain the

profiles of resonance doublet lines formed in bipolar winds that may be present in symbiotic stars.

In Section 2, we briefly describe the Sobolev theory and the basic atomic physics concerning the resonant doublet lines. We also present the kinematic stellar wind model adopted in this work and the Monte Carlo procedure. Our results are presented in Section 3. Finally, we summarise and discuss our results and observational implications in Section 4.

## 2 WIND MODEL AND CALCULATIONS

### 2.1 The Sobolev Theory

In the case of the stellar wind around the white dwarf component in a symbiotic star, the wind is highly ionised and characterized by the thermal speed  $\sim 10 \text{ km s}^{-1}$  and the bulk speed of order  $10^3 \text{ km s}^{-1}$  (Girard & Wilson 1987). We may apply the Sobolev approximation to describe the radiative transfer, if the acceleration of the wind material occurs in a small region where there are no considerable changes in physical quantities. We will check the validity of the Sobolev approximation later in detail.

When a scattering medium is of moderate column density, wing scatterings can be safely neglected. In this case, the scattering cross section associated with a resonance line photon can be well-approximated by the Dirac  $\delta$ -function with the strength  $f_{abs}(\pi e^2/m_e c)$ , or

$$\sigma_\nu = f_{abs} \frac{\pi e^2}{m_e c} \delta(\nu - \nu_0), \quad (1)$$

where  $f_{abs}$  is the absorption oscillator strength associated with the resonance transition and the frequency  $\nu$  is measured in the rest frame of the scattering atom. Therefore, a scattering occurs only when the resonance condition is met. Because of the local thermal motion, the physical width of the scattering region of a photon is given by the width where the difference of velocity is of order the thermal velocity  $v_{th}$ , that is,  $\Delta r \sim v_{th}(dv/dr)^{-1}$ .

Noting that the local velocity distribution of scattering atoms is given by the Maxwell-Boltzmann distribution, a straightforward computation gives the Sobolev optical depth  $\tau_{Sob}$  for a given direction,

$$\begin{aligned} \tau_{Sob} &= n_i \int \sigma dv c / [v(dV/ds)] \\ &= n_i f_{abs} \lambda_0 \left( \frac{\pi e^2}{m_e c} \right) \left( \frac{dV}{ds} \right)^{-1}, \end{aligned} \quad (2)$$

where  $s$  is the distance along the photon propagation direction,  $\lambda_0$  represents the resonance wavelength, and  $n_i$  is the ion number density. A more complete and detailed description of the Sobolev theory can be found in the literature (e.g. Sobolev 1947, Rybicki & Hummer 1978, Lee & Blandford 1997, Ahn, Lee & Lee 2000).

In this work, we are particularly interested in the resonance doublets, where the doublet separation is smaller than the wind velocity. Those doublets include C IV  $\lambda\lambda 1548, 1551$ , N V  $\lambda\lambda 1239, 1243$ , and O VI  $\lambda\lambda 1032, 1038$ , which are known to be prominent in symbiotic stars from observations made with space instruments such as *IUE*, the *Hopkins Ultraviolet Telescope (HUT)*, and the *Orbiting and Retrievable*

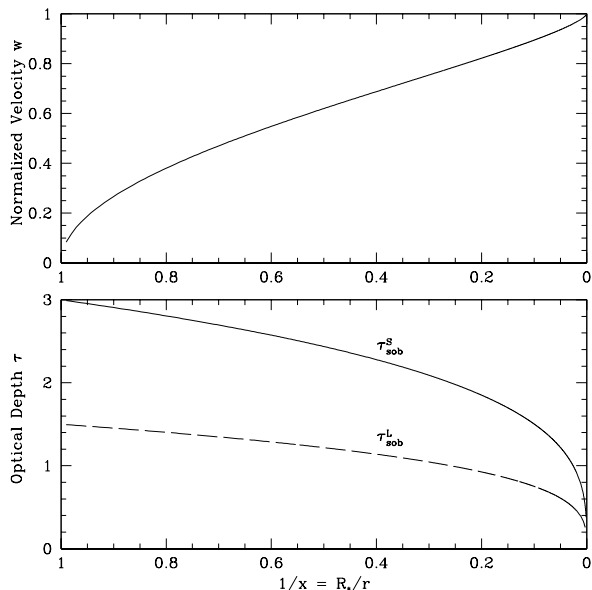


**Figure 1.** The velocity field normalized by the terminal velocity and the corresponding Sobolev optical depth  $\tau_{Sob}$  according to the distance normalized by  $R_*$ , the radius of the photosphere of the hot white dwarf. Solid and dashed lines represent the Sobolev optical depths of the short and the long wavelength components of the resonance doublets, respectively

*Far and Extreme Ultraviolet Spectrometer (ORFEUS)*. The  $S_{1/2} - P_{3/2}$  transition corresponding to the short wavelength component has the twice stronger oscillator strength than the  $S_{1/2} - P_{1/2}$  transition for the long wavelength component. Therefore, at the same position, the Sobolev optical depth  $\tau_{Sob}^S$  corresponding to the short wavelength component is also twice the optical depth  $\tau_{Sob}^L$  for the long wavelength component as are shown in Fig. 1. From now on, we refer the Sobolev optical depth  $\tau_{Sob}$  to be  $\tau_{Sob}^S$  when we do not specify the transition.

## 2.2 Kinematics of the Fast Stellar Wind

The existence of fast stellar winds with speed  $v \sim 10^3 \text{ km s}^{-1}$  around a white dwarf has been known in many white dwarf systems including the central stars of planetary nebulae (e.g. Cerruti-Sola & Petrino 1989). Many P Cygni profiles formed in fast stellar winds have been successfully fitted using a velocity law  $v(r) = v_\infty(1 - r/R_*)^\beta$  with the Sobolev approximation (Lamers, Cerruti-Sola & Perinotto 1987), where the stellar wind is assumed to start at the photospheric radius  $R_*$ ,  $\beta$  is a dimensionless parameter and  $v_\infty$  is the terminal velocity. We scale the physical distance with  $R_*$  so that the distance  $r$  from the stellar centre is obtained from the dimensionless parameter  $x$  defined by

$$x = r/R_*. \quad (3)$$

The stellar wind in this work is assumed to be steady and have geometry in the form of a bipolar cone including the spherically symmetric case. The velocity  $\mathbf{v}(\mathbf{r})$  of the wind increases monotonically outward and asymptotically approaches the terminal speed  $v_\infty$ . Although the exact

model of the velocity law in symbiotic stars is unknown, Castor, Abbott & Klein (1975) proposed a very steep velocity law for a radiation-driven stellar wind. We measure the wind velocity with the terminal speed, and introduce a dimensionless velocity  $w$  defined by

$$\mathbf{w} = \mathbf{v}/v_\infty. \quad (4)$$

Instead of assuming a wind velocity law, we prescribe the Sobolev optical depth by

$$\tau_{Sob} = \tau_0 \left( \frac{r}{R_*} \right)^{-\epsilon} = \tau_0 x^{-\epsilon}, \quad (5)$$

where  $\tau_0$  is the initial Sobolev optical depth at the wind base and  $\epsilon$  is a dimensionless positive number. We choose  $\epsilon$  to be small, so that the Sobolev optical depth does not decrease significantly in most of the wind region. This will enhance the effect of double scattering, where continuum photons blueward of the  $S_{1/2} - P_{3/2}$  transition may get scattered by the transition  $S_{1/2} - P_{1/2}$  further downstream of the wind. We use the initial Sobolev optical depth  $\tau_{Sob,0}^S = 3$ ,  $\tau_{Sob,0}^L = 1.5$  for the short and the long wavelength components of the doublet.

The density profile  $n(r)$  is obtained from the mass flux conservation assuming the constant mass loss rate  $\dot{M}$ ,

$$n(r) = \frac{\dot{M}}{4\pi m_p r^2 v(r) c_f} \propto \frac{1}{r^2 v(r)}, \quad (6)$$

where  $m_p$  is the proton mass and  $c_f$  is the covering factor of the wind normalized by the whole sky. From Eqs. (2), (5) and (6), the velocity law of the wind is given by

$$\mathbf{v}(r) = v_\infty \left[ 1 - \left( \frac{r}{R_*} \right)^{-1+\epsilon} \right]^{1/2} \hat{\mathbf{r}}. \quad (7)$$

In order to check the validity of the Sobolev approximation, we consider the length scale over which the bulk velocity changes by the amount of  $v_{th}$ ,

$$\begin{aligned} L_{Sob} &\equiv \frac{v_{th}}{dv/dr} \\ &= 2R_* \frac{v_{th}}{v_\infty} (1-\epsilon)^{-1} \left( \frac{r}{R_*} \right)^{2-\epsilon} \left[ 1 - \left( \frac{r}{R_*} \right)^{-1+\epsilon} \right]^{1/2}. \end{aligned} \quad (8)$$

We note that  $v_{th}/v_\infty \leq 10^{-2}$ , and therefore  $L_{Sob} \leq 0.02R_* x^{2-\epsilon}$ . This implies that  $L_{Sob}$  can be comparable to  $R_*$ , when  $x \geq 10$  and  $\epsilon = 0.3$ . When  $x$  is small, the density changes steeply near  $R_*$ , and  $L_{Sob} \ll R_*$  validating the use of the Sobolev approximation. When  $x$  gets larger, the density variation is almost scale-free, which also makes the Sobolev approximation reliable.

The mass loss rate is related to the Sobolev optical depth  $\tau_{Sob}$  by

$$\dot{M} = 5.1 \times 10^{-12} \tau_0 (1-\epsilon) c_f \left( \frac{v_\infty}{10^3 \text{ km s}^{-1}} \right)^2 M_\odot \text{ yr}^{-1}, \quad (9)$$

and the hydrogen number density can be obtained by

$$\begin{aligned} n(r) &= 1.6 \times 10^7 \tau_0 (1-\epsilon) x^{-2} w^{-1} \\ &\times \left( \frac{R_*}{10^{11} \text{ cm}} \right)^{-2} \left( \frac{v_\infty}{10^3 \text{ km s}^{-1}} \right) \text{ cm}^{-3}. \end{aligned} \quad (10)$$

According to the study of Cerruti-Sola & Perinotto (1989), the terminal velocities of the fast winds in many planetary nebulae range  $1000 - 2500 \text{ km s}^{-1}$ . Vogel & Nussbaumer (1994) also showed that the fast wind in the symbiotic star AG Peg is about  $1000 \text{ km s}^{-1}$ . In this study,

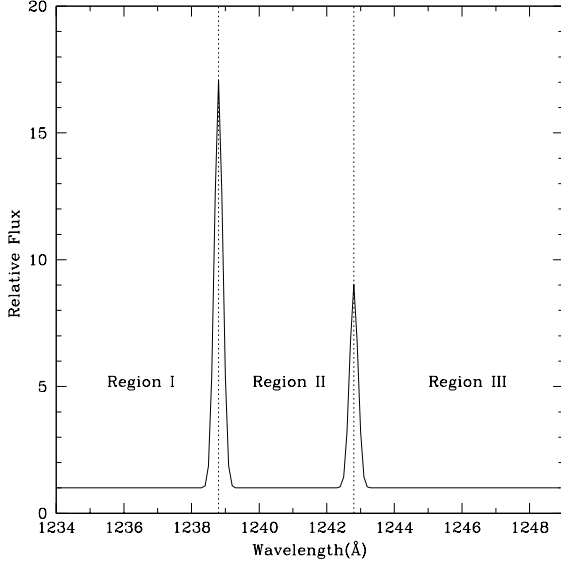


**Figure 2.** The spectrum of the source that consists of a flat continuum and resonance doublet lines, which we assume is N v here. We used Gaussian profiles for the line doublet whose equivalent widths are 5 Å and 2.5 Å for the short and the long wavelength components, respectively. The velocity dispersion is chosen to be  $\sigma = 30 \text{ km s}^{-1}$  for both components. The wavelength regions are divided according to the wavelength relative to the resonance line centres of the doublet.

we choose the doublet separation to be  $960 \text{ km s}^{-1}$  corresponding to the N v doublet and set the terminal velocity  $v_\infty = 3000 \text{ km s}^{-1}$  in order to investigate the effect of double scattering. Therefore, we focus on the profiles formed by various scatterings, not on the full dynamical range of the wind.

With the choices of the parameters  $\epsilon = 0.3$ ,  $\tau_0 = 3$  and the wind half opening angle  $30^\circ$ , the mass loss rate  $\dot{M} = 1.3 \times 10^{-11} M_\odot \text{ yr}^{-1}$ . It is notable that the mass loss rate is compatible to those of Michalitsianos et al. (1988) which are  $4.5 \times 10^{-12} \leq \dot{M} \leq 1.0 \times 10^{-11} M_\odot \text{ yr}^{-1}$  for R Aqr and  $1.5 \times 10^{-11} \leq \dot{M} \leq 3.1 \times 10^{-11} M_\odot \text{ yr}^{-1}$  for RX Pup. According to them, it is estimated that the momentum flux from the red giant is about 200 times greater than that from the hot companion. The corresponding mass loss rate from the red giant is  $1.3 \times 10^{-7} M_\odot \text{ yr}^{-1}$  which is consistent with the calculation by Vogel & Nussbaumer (1994).

The profiles of the wind velocity and the Sobolev optical depth are shown in Fig. 1 as a function of the normalized distance  $x$ .

### 2.3 The Sobolev Monte Carlo Code

Firstly, we consider the volume emission measure in the stellar wind region. The relevant quantity to be considered is

$$\begin{aligned} \int n(r)^2 dV &= n_0^2 R_*^3 \tau_0^2 (1 - \epsilon)^2 4\pi \int_1^\infty \frac{dx}{x^2 - x^{1+\epsilon}} \\ &= n_0^2 R_*^3 \tau_0^2 (1 - \epsilon)^2 4\pi f(\epsilon), \end{aligned} \quad (11)$$

where  $n_0 = 1.6 \times 10^7 \text{ cm}^{-3}$  and  $f(\epsilon) \equiv \int_1^\infty \frac{dx}{x^2 - x^{1+\epsilon}}$  which is a steep function of  $\epsilon$  near zero. For a small value

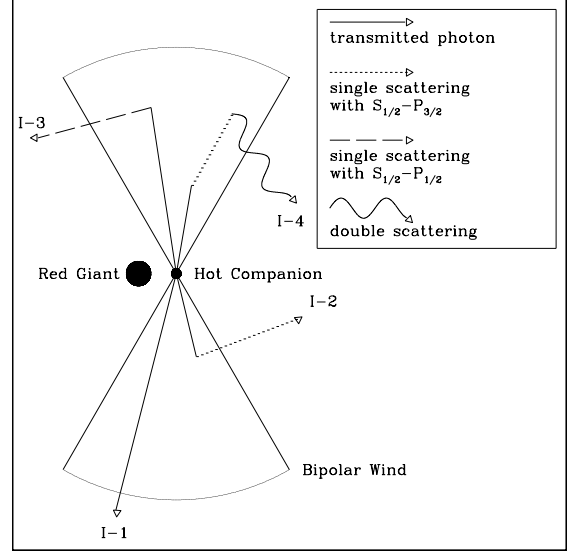


**Figure 3.** Conceptual diagram for single resonance scatterings and double resonance scatterings. The solid, dotted, dashed and wavy lines represent no scattering, single scattering resonant with  $S_{1/2} - P_{3/2}$ , single scattering resonant with  $S_{1/2} - P_{1/2}$  and double scattering, respectively. The indices represent possible scatterings that a given photon in Region I can suffer.

$\epsilon = 0.3$ , we also have a moderate value of  $f(\epsilon)$  and the quantity  $n^2 V$  is basically determined by  $n_0^2 R_*^3 \simeq 10^{47} \text{ cm}^{-3}$  much smaller than typically observed in symbiotic stars (e.g. Proga, Kenyon & Raymond 1998). Therefore, if we consider the wind as a photon scattering region, almost all the photons are generated near the hot star component. This means that the photon source is separated from the wind.

From this consideration, we prepare a photon source near the white dwarf component, from which both continuum photons and line photons are injected into the wind region. We choose the equivalent width of the short wavelength component to be 5 Å and 2.5 Å for the long wavelength component. This ratio corresponds to the optically thin limit of the emission plasma. Without specifying the details of the kinematics of the emission region, we just assume that the line profile is given by a Gaussian with the velocity dispersion  $\sigma = 30 \text{ km s}^{-1}$  for both components. Fig. 2 shows the profile of the incident photon flux that is injected into the wind region.

According to the wavelength relative to the two resonance line centres, we conceptually divide the injected photons into three categories, which we call Region I, II and III shown in Fig. 2.

For photons in Region III, there is no point in the wind where the resonance condition can be satisfied for either transition. Therefore, no photons in Region III will be scattered in the wind in our model. Photons from Region II can only be resonantly scattered in the wind with the  $S_{1/2} - P_{1/2}$  transition, for which the relevant Sobolev optical depth is  $0.5\tau_{Sob}$ .

Most complicated interactions can be seen for photons in Region I, because they can be first resonantly scattered with the  $S_{1/2} - P_{3/2}$  transition and can be additionally scat-

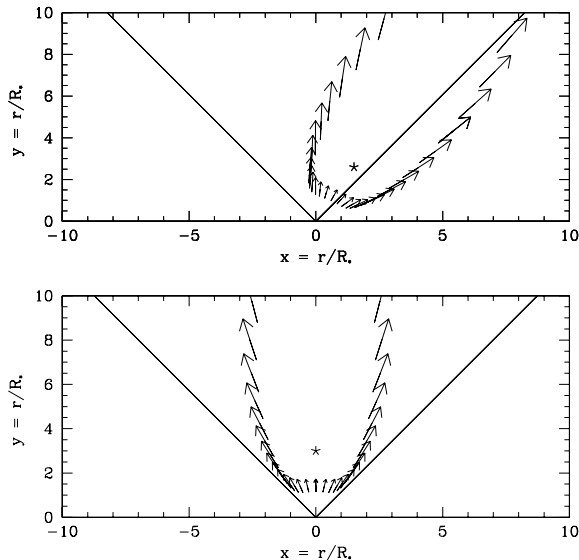


**Figure 4.** Examples of the Sobolev surfaces for double scattering in the  $x - y$  plane. A given photon is resonantly scattered at the position marked by an asterisk, and the surfaces with the velocity component equal to the doublet separation. The arrows and the solid lines represent the velocity vectors at the positions and the wind region, respectively.

tered with the  $S_{1/2} - P_{1/2}$  transition. Hence there are four cases that can occur for photons in Region I. The first case denoted by I-1 in Fig. 3 corresponds to the escape without any scattering. The second case (I-2) represents the escape after a resonance scattering associated with  $S_{1/2} - P_{3/2}$  transition. The third case (I-3) corresponds to the escape after a resonance scattering associated with  $S_{1/2} - P_{1/2}$  transition. The final case (I-4) is the double scattering, where a given photon escapes from the bipolar wind after resonance scatterings associated with both transitions. Fig. 3 illustrates these four possible cases.

We consider the Sobolev surface, which is defined as the collection of those points moving away from a given point with the same velocity component along the line of the photon propagation. In order to describe doubly scattered photons, we have to consider the Sobolev surface moving away with the velocity of the doublet separation from a given point where the first resonance scattering occurs. For illustration, in Fig. 4 we show a couple of Sobolev surfaces for double scattering in  $x - y$  plane, where the given photon is firstly resonantly scattered at the positions marked by an asterisk. The Sobolev optical depth  $\tau_{Sob}^D$  associated with this double scattering is given by

$$\begin{aligned} \tau_{Sob}^D &= n_i f_{abs}^L \lambda_0 \left( \frac{\pi e^2}{m_e c} \right) |\hat{\mathbf{n}} \cdot (\hat{\mathbf{n}} \cdot \nabla) \mathbf{V}|^{-1} \\ &= n_i f_{abs}^L \lambda_0 \left( \frac{\pi e^2}{m_e c} \right) \left| (\hat{\mathbf{n}} \cdot \hat{\mathbf{r}})^2 \frac{dV}{dr} + \frac{V}{r} [1 - (\hat{\mathbf{n}} \cdot \hat{\mathbf{r}})^2] \right|^{-1}, \quad (12) \end{aligned}$$

where  $\hat{\mathbf{n}}$  is the photon wave vector before double scattering and  $f_{abs}^L$  is the oscillator strength corresponding to the  $S_{1/2} - P_{1/2}$  transition.

In Fig. 5, we show the inverse of the velocity gradient

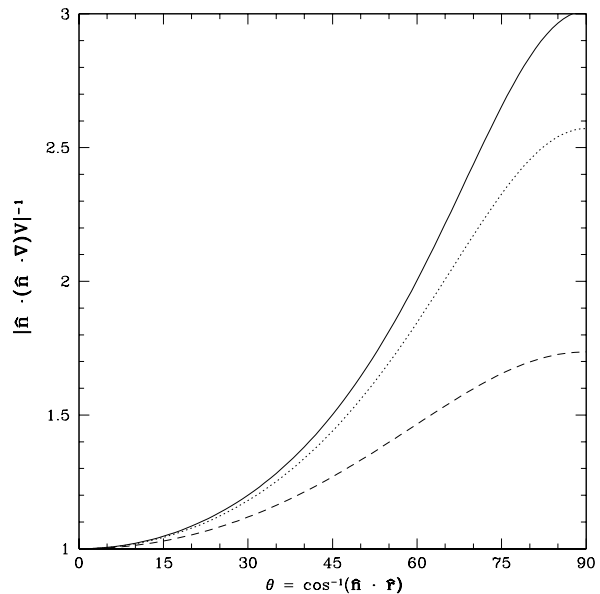


**Figure 5.** The dependence of the Sobolev optical depth  $\tau_{Sob}$  on the photon propagation direction at a given position. The horizontal axis represents the angle between the incident photon wavevector and the radial or the wind direction. The solid, dotted and dashed lines represent the inverse of the velocity gradient at  $x=1.16, 1.2$  and  $1.3$  which are normalized by the inverse value of the velocity gradient for the radial direction.

for various directions at three positions  $x = 1.16, 1.2, 1.3$  in order to find the dependence of  $\tau_{Sob}^D$  on the photon propagation direction. We can see that  $\tau_{Sob}^D$  may vary by a factor of three dependent on the direction.

Since we are particularly interested in bipolar winds, which may be related with the bipolar nebular morphologies known in a number of symbiotic stars (e.g. Corradi 1995, Corradi & Schwarz 1993), it is natural to expect that there exists a very thick circumstellar component in the equatorial plane. Therefore, in our model, we introduce an opaque medium outside the photon source and the wind base. For simplicity, we set the physical size of the opaque medium to be  $x = 1.01$ , so that observer in the polar direction can see the wind base, which is hidden from the equatorial direction.

We typically inject  $10^5$  continuum photons in a bin with  $\Delta\lambda = 0.1 \text{ \AA}$ . The injection number is adjusted near the doublet line centres so that the line features possess the equivalent widths of  $5 \text{ \AA}$  and  $2.5 \text{ \AA}$  and the Gaussian profiles with velocity dispersion  $\sigma = 30 \text{ km s}^{-1}$ . We collect emergent photons according to the direction cosine of the wave vector with a bin size of  $\Delta\mu = 0.1$ , and the wavelength bin  $\Delta\lambda = 0.023 \text{ \AA}$  corresponding to the thermal width of  $T = 10^4 \text{ K}$ . In our simulations, we normalize the relevant quantities to those associated with N v  $\lambda\lambda 1238.8, 1242.8$ .

### 3 RESULTS

We investigate the dependence of the profiles on the observer's line of sight, the mass loss rate, the wind half opening angle and the existence of the opaque circumstellar region.

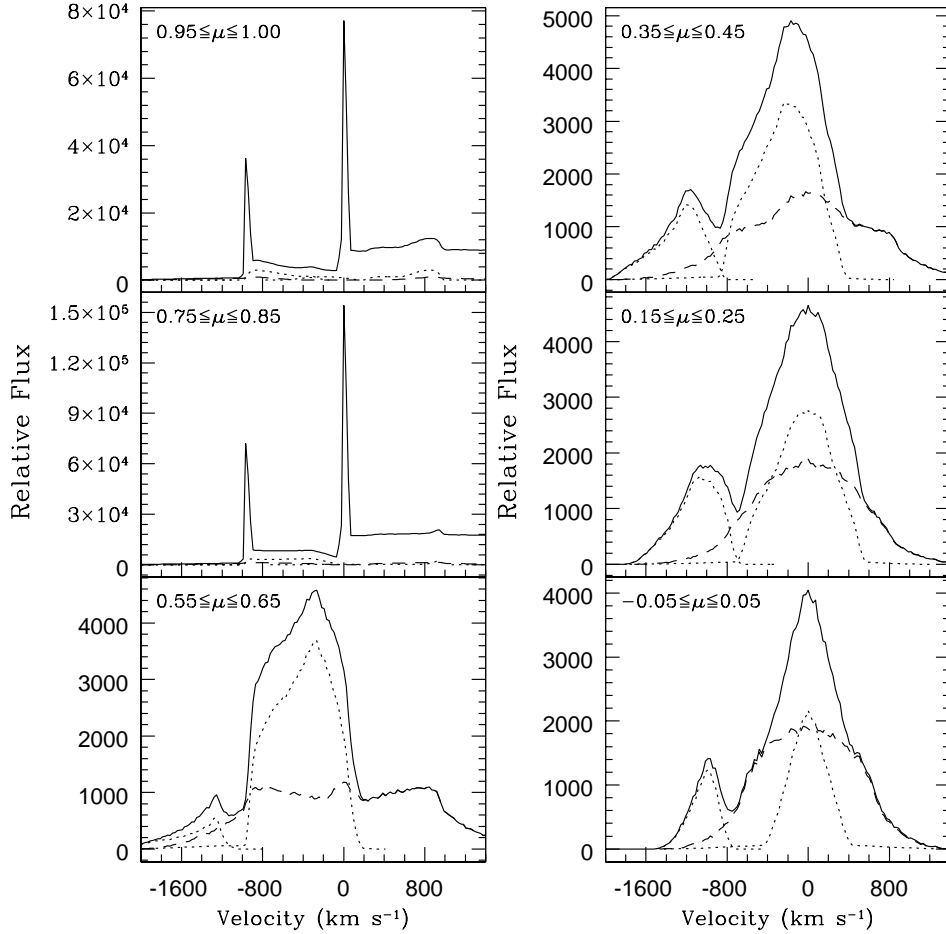


**Figure 6.** Profiles according to the various observer's lines of sight. The number of photons counted in each observer's line of sight is referred to the relative flux and is shown as a solid line. The dotted and dashed lines mean the number of photons which suffered single scattering and the double scattering, respectively. The wind half opening angle is set to be  $45^\circ$ .

### 3.1 Profiles for Various Lines of Sight

We first fix the wind half opening angle to be  $45^\circ$  and consider the variation of the profiles dependent on the observer's line of sight. Fig. 6 shows our result, in which we find significant difference in the profiles viewed from the polar direction and from the equatorial direction.

When  $\tau_{Sob}$  is much larger than 1 and the observer is in the polar direction, we normally obtain P Cygni type profiles. However, when the Sobolev optical depth  $\tau_{Sob}$  is moderate ( $\tau_{Sob} \simeq 1$ ), the observer sees profiles characterized by two narrow peaks. The blue part of the short wavelength peak is obtained from suppression of the incident flux by a factor  $e^{-\tau_{Sob}(r_1) - 0.5\tau_{Sob}(r_2)}$  with  $r_1$  and  $r_2$  being the locations of the resonance transitions with  $S_{1/2} - P_{3/2}$  and  $S_{1/2} - P_{1/2}$ , respectively. In contrast, the red part of the short wavelength peak and the blue part of the long wavelength peak are suppressed by a factor  $e^{-0.5\tau_{Sob}(r_3)}$ , where  $r_3$  is the location of the resonance scattering with  $S_{1/2} - P_{1/2}$ . Therefore the double scattering process affects the doublet line ratio significantly. In our model, only the blue part of the long wavelength component can satisfy the resonance condition and be affected by the wind. Hence we observe the

fairly stronger long wavelength component than the short wavelength. This is interesting considering the *IUE* spectra of RX Pup and R Aqr which were pointed out by Michalitsianos et al. (1988). According to them, in RX PUP and R Aqr the C IV doublet showed anomalous line ratio in the blue part only, where the short wavelength component is weaker than the long wavelength component. However, in the red part, the doublet flux ratio almost restores the optically thick limit of 1:1. Therefore, it is very probable that the doublet line ratio in the blue part may be affected by extrinsic components including the fast outflowing wind.

As is apparent from Fig. 6, the continuum blueward of the short wavelength component (Region I in Fig. 2) is weaker than that for Region II, which is again weaker than that for Region III. A similar trend is observed for  $\mu \geq 0.85$  (in the direction of the wind region). However, qualitatively different profiles are obtained for  $\mu \leq 0.65$ , for which the observer is outside the wind flowing direction.

If we see symbiotic stars outside the wind flowing direction ( $\mu \leq 0.65$  in Fig. 6), the emergent profiles are composed of only scattered photons and no transmitted continuum can be seen. One of the most interesting features of this bipolar wind system is shown for  $\mu \simeq 0$ , where we see the clear

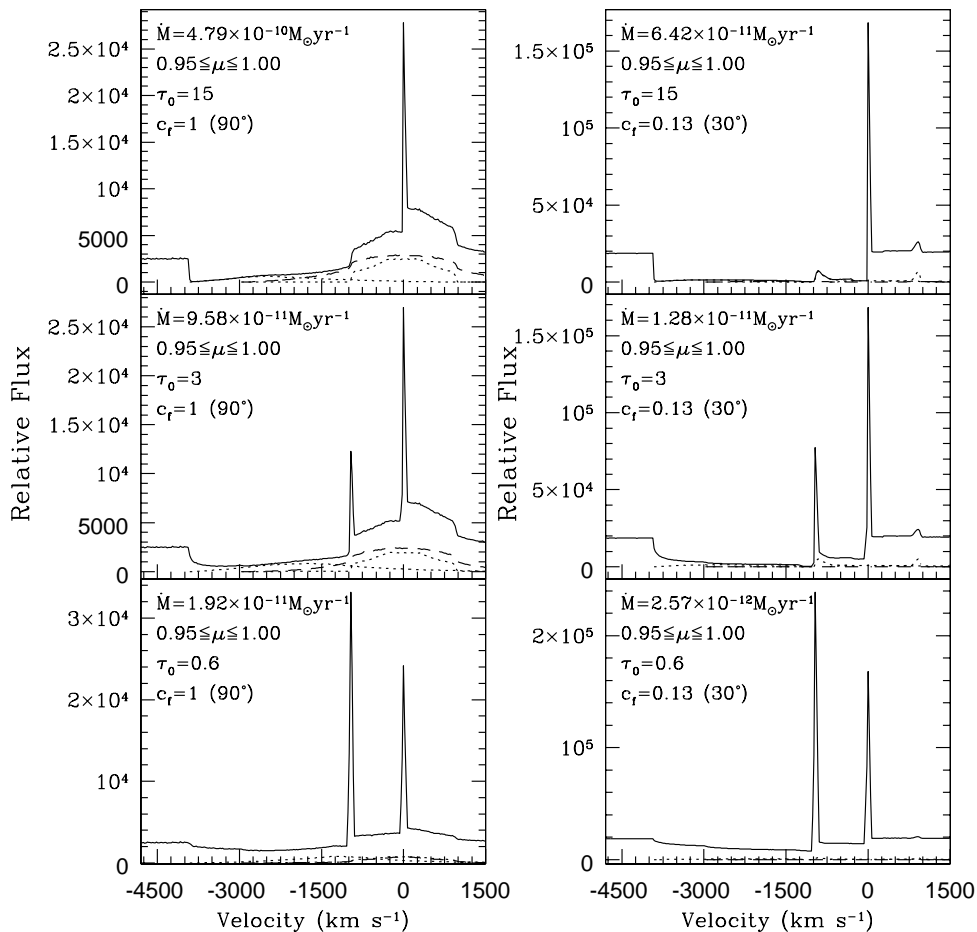


**Figure 7.** Profiles for various mass loss rates  $\dot{M}$ . We fix the observer’s line of sight to be in the polar direction. The profiles shown in the left correspond to spherical winds. In the right part are shown the profiles for bipolar winds with the half opening angle  $30^\circ$ . The mass loss rates are chosen so that the initial Sobolev optical depth  $\tau_0 = 0.6, 3$  and  $15$  and  $c_f$  represents the covering factor of the wind with respect to the photon source. The various lines represent the same quantities illustrated in Fig. 6

effect of the photon redistribution by the double scattering process. The net effect of double scattering is to take out the flux of the short wavelength component and redistribute it around the long wavelength component. Therefore, the flux around the long wavelength component increases.

More quantitatively, the ratio of the fluxes contributed by single scatterings at the short and the long wavelength components and double scattering to the total flux is given by 15%, 39% and 46% in the particular case  $0.15 \leq \mu \leq 0.25$  in Fig. 6. This means that more than half of 1239 photons are doubly scattered and converted into 1243 photons. It is notable that the profile around the long wavelength component gets greater dispersion than the dispersion that would be obtained in the case when only single scattering at the long wavelength component is operational. This is because doubly scattered photons acquire the Doppler shift corresponding to the doublet separation in addition to the Doppler shift for the velocity at the scattering point. Therefore, the doublets in a bipolar wind are characterized by the inverted flux ratio and much broadened profiles of the long wavelength component.

### 3.2 Dependence on the Mass Loss Rate

In order to investigate the dependence of the profiles on the mass loss rate  $\dot{M}$ , we set the covering factor of the wind to be 1 and 0.13 corresponding to the spherical and bipolar winds with half opening angles  $90^\circ$  and  $30^\circ$ , respectively. In this subsection, we fix the observer’s line of sight to be the polar direction.

According to the various mass loss rates, considerably different profiles are obtained as shown in Fig. 7. The mass loss rate is proportional to the initial optical depth  $\tau_0$  as in Eq. (9). Various doublet line ratios are obtained because the peaks of the resonance doublet are sensitive to  $\tau_0$ . For the spherical wind, the Sobolev surface for double scattering at a given position subtends a fairly large solid angle, and therefore the emergent flux profile will be significantly affected by photons redistributed by double scattering. In particular, when the mass loss rate is very high (the top-left panel of Fig. 7), the suppression of the short wavelength component is so large that no apparent line feature is found around at  $1238.8 \text{ \AA}$ . Furthermore, all the photons blueward of the  $S_{1/2} - P_{3/2}$  resonance are redistributed in frequency space up

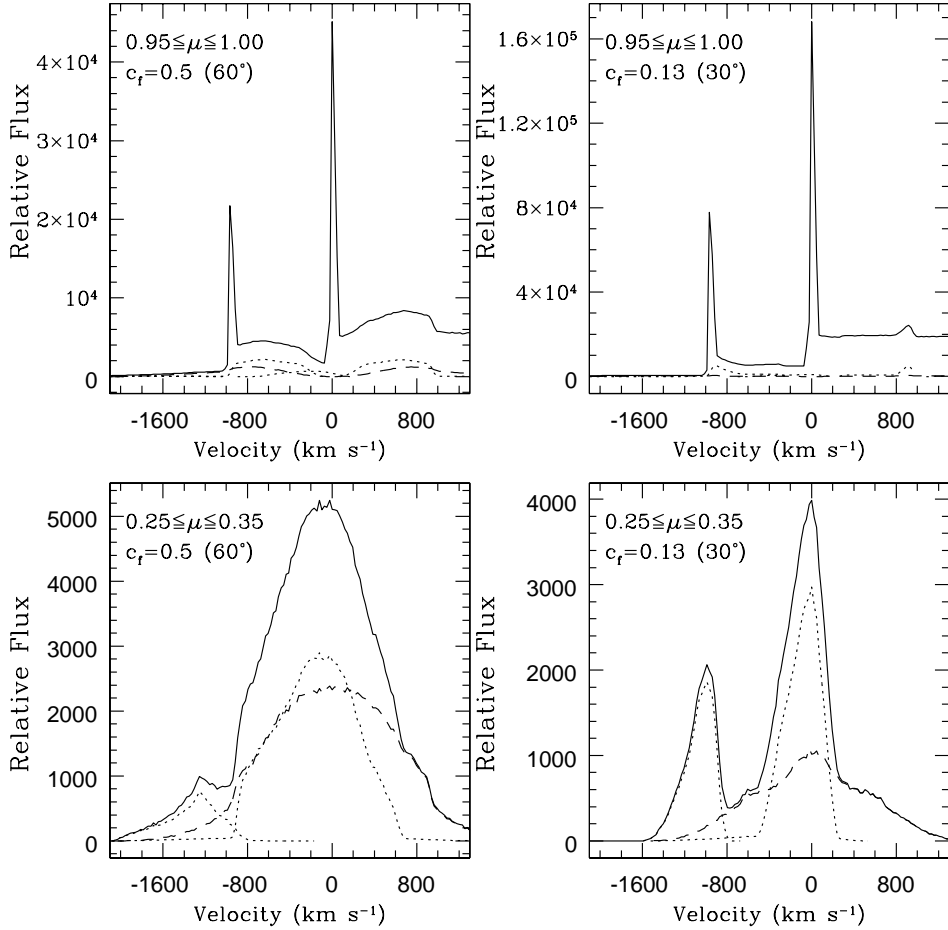


**Figure 8.** The profiles for the wind with half opening angle  $60^\circ$  and  $30^\circ$ . The various lines represent the same quantities illustrated in Fig. 6

to the wind terminal speed and form the strong and broad component around the  $S_{1/2} - P_{1/2}$  resonance wavelength.

However, for the narrow bipolar winds, the Sobolev surface for double scattering has a small solid angle, where we expect a negligible contribution from doubly scattered photons. Since the scattering process in the bipolar wind can be effectively regarded as a photon annihilation process from the observer's line of sight, we see a quick disappearance of the broad components around the doublet formed by the photons redistributed by single scattering.

### 3.3 Dependence on the Wind Opening Angle

We briefly investigate the profile dependence on the wind opening angle in order to study the profile formation in a bipolar wind. As a reference, the profile from a spherical wind can be found in Fig.7. The inverted intensity ratio will be sensitively dependent on the mass loss rate. Around the line centres, there appear broad bases which are formed by those photons redistributed from single resonant scatterings associated with  $S_{1/2} - P_{1/2,3/2}$  transitions, and also contributed from double resonant scatterings of photons initially generated in Region I.

In Figs. 8, we generated profiles for bipolar winds with

half opening angles  $60^\circ$  and  $30^\circ$ , respectively. We chose two lines of sight for illustration. The overall trend is explained in the previous subsection. As the half opening angle decreases, the redistributed photons contribute less to the profile formation. This effect is clearly seen in the case  $0.25 \leq \mu \leq 0.35$ , for example. In a bipolar wind with  $60^\circ$  half opening angle, we can barely recognise the short wavelength component, whereas the long counterpart is enhanced significantly. In this case, there is effectively one broad line component that is centred nearly at  $1242.8 \text{ \AA}$ , slightly blueward of the long wavelength component. However, in the case of the  $30^\circ$  bipolar wind, there appear two clear line components of which the longer one is the stronger. The contribution of redistributed photons is significantly suppressed. The long wavelength component is, however, broader than the short wavelength component and there is also a broad base redward of the long wavelength component.

The fluxes observed from the equatorial direction display various profiles that are not of a P Cygni type. These various profiles are typified by inverted line ratios, and are formed by photons redistributed by single and/or double scatterings, which play an essential role in profile formation.

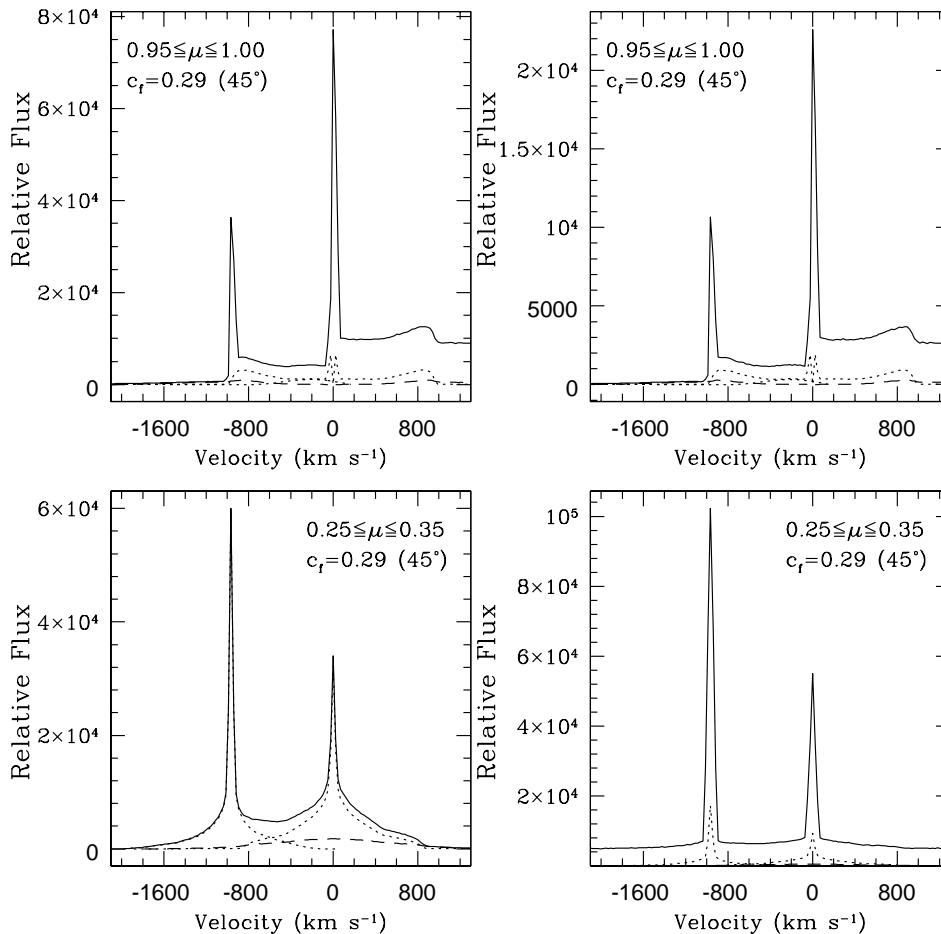


**Figure 9.** Profiles for the cases where the opaque media are changed. In the left, the opaque media are shrunk to hide only the photon injecting source and the wind base is fully seen from all directions. The opaque media are completely removed in the right, so that the photon injecting source and the wind base are fully seen. The wind half opening angle is set to be  $45^\circ$ . The various lines represent the same quantities illustrated in Fig. 6

### 3.4 Miscellaneous Cases

In Fig. 9, we shrink the opaque component, so that it only hides the photon source. By doing this, effectively we consider the case where the wind base part is fully seen from any directions.

When an observer is in the polar direction, we get the same result as before. However, from the equatorial direction we obtain different profiles to which the wind base part contributes additionally with very small Doppler shifts. For the equatorial viewer, the wind base part actually acts as a narrow line source which is almost at rest. Therefore, the qualitative difference is due to the addition of the narrow line component to the broad scattered profiles.

Finally, when we remove the opaque component (Fig. 9), then we see fully the source and the scattering wind. No discernible difference is found for profiles observed from the polar direction. For an observer in the equatorial direction, the profile is dominantly that of the source and modified in a very small amount by scattered components.

## 4 DISCUSSION AND SUMMARY

In this paper we investigate the doublet resonance line formation in bipolar conic flows in symbiotic stars by adopting the Sobolev Monte Carlo method. We also pay special attention to the doublet line ratios.

When an observer is in the polar direction, there appear two peaks at the line centres coinciding with those of the resonance doublets. This is because we chose the mass loss rate  $\dot{M}$  so that the Sobolev optical depth  $\tau_{Sob} \simeq 1$  for most of the velocity space, and therefore the line flux of the short component is suppressed by a factor  $e^{-\tau_{Sob}} \simeq 0.3$ . The red part of the long wavelength peak does not suffer any suppression. This fact implies that the detailed peak profiles differ in a systematic way. The suppression pattern also repeats for continuum parts, where the weakest occurs blueward of the short wavelength peak.

Michalitsianos et al. (1988) investigated the profiles of  $C\text{ IV } \lambda\lambda 1548, 1551$  in the symbiotic stars RX Pup and R Aqr, from which they found the weaker short wavelength component than the long wavelength component. They particularly noted that the profiles are characterized by significant sup-

pression in the blue part of the short wavelength peak. The peak flux ratio is most sensitively dependent on the Sobolev optical depth, particularly when  $\tau_{Sob} \simeq 1$  and is insensitive on the covering factor of the wind.

In RX Pup and R Aqr, there may exist a scattering component outflowing with speed less than the doublet separation. In this case, only single scattering is operational, which can cause the deviations of the doublet line ratio from the optically thin limit. However, when double scattering is possible, much more various doublet line ratios can be produced. It is uncertain that there exists an outflow moving faster than the doublet separation of  $500 \text{ km s}^{-1}$  in RX Pup and R Aqr. In order to find the concrete evidence of double scattering, we need to obtain spectra with sufficient quality to discern the continuum level which are contributed by the redistributed photons.

When we observe in the equatorial direction, we find that the profiles are characterized by two broad components, where the long wavelength component is the broader and stronger of the two. This qualitative feature does not change even if we vary either the mass loss rate or the Sobolev optical depth  $\tau_{Sob}$  as long as  $\tau_{Sob}$  exceeds unity. However, when the observer is in the polar direction, various P Cygni type profiles are obtained dependent on the mass loss rate. We believe that the bipolarity of the stellar wind is mainly responsible for these spectroscopic characteristics.

It is quite interesting that the symbiotic nova AG Peg shows the profiles of N v and C iv in the hot wind phases similar to those obtained in this work. We strongly believe that the hot wind in AG Peg takes the bipolar form with the speed exceeding  $10^3 \text{ km s}^{-1}$ . Kenny, Taylor & Seaquist (1991) used the Very Large Array (VLA) in order to investigate the morphological structure of AG Peg. They found a bipolar outer nebula extending  $\sim 40''$ . They also found a bipolar enhancement in the inner nebula having a subarc-second extent, which is consistent with the existence of a bipolar wind. However, it should also be noted that Nussbaumer, Schmutz & Vogel (1995) reported a P Cygni type absorption in N v in AG Peg using the *Hubble Space Telescope*.

Most symbiotic stars are not optically resolved and therefore their morphology is very uncertain. In planetary nebulae, it is still highly controversial whether the binarity of the central star system can be linked to the bipolarity of the nebula (e.g. Morris 1987, Livio & Soker 1988, Soker 1998). A significant input should be provided from the morphological study of symbiotic stars. In this respect, it is proposed that the resonance doublets can be a useful diagnostic of the bipolar winds in symbiotic stars.

## ACKNOWLEDGMENTS

J.J.Y. is grateful to Chan-Gyung Park for useful discussions and indebted to Myungshin Im for encouragement for this research work. This work was supported by Korea Research Foundation Grant (KRF-2001-003-D00105).

## REFERENCES

Ahn S.-H., Lee H.-W., 2002, in preparation.

- Ahn S.-H., Lee H.-W., Lee H. M., 2000, *Journal of the Korean Astronomical Society*, 33, 29
- Castor J. I., Abbott D. C., Klein R. I., 1975, *ApJ*, 195, 157
- Corradi R., 1995, *MNRAS*, 276, 521
- Corradi R., Schwarz H., 1993, *A&A*, 267, 714
- Cerruti-Sola M., Perinotto M., 1989, *ApJ*, 345, 339
- Ezuka H., Ishida M., Makino F., 1998, *ApJ*, 499, 388
- Feibelman W. A., 1983, *A&A*, 122, 335
- Girard T., Wilson L.A., 1987, *A&A*, 183, 247
- Harries T. J., Howarth I. D., 1996, *A&AS*, 119, 61
- Iben I. J., Tutukov A. V., 1996, *ApJS*, 105, 145
- Kenny H. T., Taylor A. R., Seaquist E. R., 1991, *ApJ*, 366, 549
- Kenyon S. J., 1986, *The Symbiotic Stars.*, Cambridge Univ. Press, Cambridge
- Lamers H. J. G. L. M., Cerruti-Sola M., Perinotto M., 1987, *ApJ*, 314, 726
- Lee H.-W., Park M.-G., 1999, *ApJ*, 515, L89
- Lee H.-W., Blandford R. D., 1997, *MNRAS*, 288, 19
- Livio M., Soker N., 1988, *ApJ*, 329, 764
- Mastrodemos N., Morris M., 1998, *ApJ*, 497, 303
- Michalitsianos A. G., Kafatos M., Fahey R. P., Viotti R., Cassatella A., Altamor A., 1988, *ApJ*, 331, 477
- Morris M., 1987, *PASP*, 99, 1115
- Mürset U., Wolff B., Jordan S., 1997, *A&A*, 319, 210
- Mürset U., Schmid H. M., 1999, *A&AS*, 137, 473
- Nussbaumer H., Schmutz W., Vogel H., 1995, *A&A*, 293, L13
- Olson G. L., 1982, *ApJ*, 255, 267
- Paczynski B., Zytokow A., 1978, *ApJ*, 222, 604
- Proga D., Kenyon S., Raymond J., 1998, *ApJ*, 501, 339
- Rybicki G. B., Hummer D. G., 1978, *ApJ*, 219, 654
- Schmid H. M., 1989, *A&A*, 211, 31
- Schmid H. M., 1996, *MNRAS*, 282, 511
- Schmid H. M. et al., 1999, *A&A*, 348, 950
- Schmid H. M., & Schild H., 1994, *A&A*, 281, 145
- Sobolev V. V., 1947, *Moving Envelopes of Stars*. Leningrad State Univ., Leningrad (English translation: 1960, Gaposchkin S., Harvard Univ. Press, Cambridge, MA)
- Soker N., 1998, *ApJ*, 496, 833
- Soker N., Rappaport S., 2000, *ApJ*, 538, 241
- Vogel M., Nussbaumer H., 1994, *A&A*, 284, 145